Prototype of a Negative-Sequence Turn-to-Turn Fault Detection Scheme for Transformers

Daniel Zacharias and Ramakrishna Gokaraju, *Senior Member, IEEE*

***Abstract*—Digital relays are capable of computing the negative-sequence current on both primary and secondary sides of the transformer along with the phase difference between these two negative-sequence currents. By using both phase and magnitude information, negative-sequence current could be used to detect minor turn-to-turn faults involving 3% of the transformer's windings or more. Turn-to-turn faults may still occur even if no current is flowing on one side of the transformer, such as during energization. With no current flowing in the secondary windings of the transformer, negative-sequence current-based algorithms become insensitive. This paper introduces a relay prototype, using both negative-sequence current and negative-sequence voltage, which retains its sensitivity during energization. The relay's performance for several commonly encountered system scenarios, such as overexcitation, current-transformer saturation, nonzero fault resistance, transformer energization, and external faults were also examined. The experimental results presented in this paper indicate that the algorithm proposed in this paper is faster and more sensitive than restrained current differential protection and is capable of detecting turn-to-turn faults occurring during transformer energization.**

***Index Terms*—Digital protection, transformer protection.**

I. Introduction

NUMEROUS techniques have been proposed in literature to detect turn-to-turn faults in power transformers. Reference [1] proposes a fuzzy logic-based technique able to detect turn-to-turn faults involving 16% of a transformer's windings while the transformer was being energized. The algorithm employed 12 criteria in order to distinguish a healthy transformer from faulted transformer. One criterion of this algorithm is based on the assumption that internal transformer faults are very unlikely to be three-phase faults.

This property of turn-to-turn faults was utilized in Reference [2] which proposes a zero-sequence current-based detection scheme. The mechanical forces of energization may stress the transformer's insulation and result in a turn-to-turn fault. The algorithm in [2] is sensitive to faults producing zero sequence current outside the transformer's zone of protection. Therefore this algorithm is intended to be used in conjunction with a current differential protection scheme in order to make it more sensitive to turn-to-turn faults during energization.

Manuscript received December 12, 2014; revised December 26, 2014 and December 26, 2014; accepted May 01, 2015. Date of publication October 12, 2015; date of current version January 21, 2016. Paper no. TPWRD-01529-2014.

The authors are with the University of Saskatchewan, Saskatoon, SK S7N 4K2 Canada (e-mail: daz692@campus.usask.ca; rama.krishna@usask.ca).

Color versions of one or more of the figures in this paper are available online at http://ieeexplore.ieee.org.

Digital Object Identifier 10.1109/TPWRD.2015.2483524

Reference [3] introduces a negative-sequence current-based algorithm capable of detecting turn-to-turn faults, involving 1% of the transformer's windings, during normal transformer operation. This algorithm makes use of the primary and secondary negative-sequence current magnitudes, along with their phase difference to detect turn-to-turn faults and reject faults external to the transformer's zone of protection. This sensitivity of the algorithm was verified in [4]. However, during transformer energization, this algorithm was found to be not suited for turn-to-turn faults detection.

During energization, the transformer's secondary breaker is open. Inrush current flows on the primary side of the transformer while no current flows on the secondary side of the transformer. Therefore, the phase information of the negative-sequence current on the secondary side of the transformer is not useful during energization.

The use of third-harmonic voltage to protect the stator windings of a generator is described in Reference [5]. This protection scheme made use of third-harmonic voltage in order to protect generator stator windings. The third-harmonic voltage magnitude present at the terminals of the winding's terminals was compared to the third-harmonic voltage magnitude present at the neutral grounding transformer. The concept of using voltage differential algorithm to protect windings was extended to a negative-sequence voltage-based algorithm (NSVA) in this work.

A faulted transformer's turns ratio is known to change due to turn-to-turn faults [6]. This transformer protection scheme is based on the changes in flux linkages which occur due to turn-to-turn faults. It was successfully applied to both Y-Y winding arrangement and Y-Δ winding arrangements. The algorithm described in [6] was also found to operate during transformer energization and overexcitation conditions. The algorithm's sensitivity was able to detect turn-to-turn faults comprised of 10% of the windings or more.

A turn-to-turn fault not only affects the currents seen at a transformer's terminals, but also the voltages. A turn-to-turn fault changes the transformer's turns ratio as turns are bypassed by the fault and the relationship between the primary and secondary flux linkages changes as described in [6]. The algorithm proposed in this paper compares the transformer's primary negative-sequence voltage magnitude to the secondary negative-sequence voltage magnitude in order to detect turn-to-turn faults during energization. When combined with the negative-sequence current-based algorithm described in [3], an algorithm was developed in order to protect the transformer during energization and normal operation. This algorithm, proposed in this paper, was prototyped and tested using a real-time simulator.

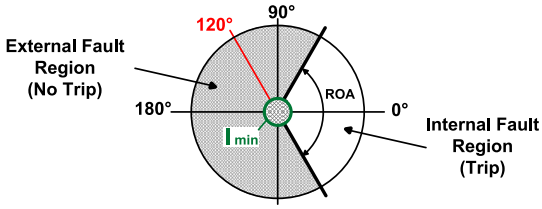

Fig. 1. Negative-Sequence Current Fault Detection.

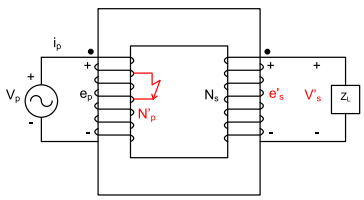

Fig. 2. Primary Side Turn-to-Turn Fault, Phase C.

In order to test the relay prototype, executing the proposed algorithm, a transformer was simulated using a real-time simulator. This transformer model, capable of simulating transformer energization current along with turn-to-turn faults, is based on Reference [7]. A single-phase transformer model is constructed using a 4-winding transformer, shown in Fig. 5, in parallel with a nonlinear reactor model. Three single-phase transformer models were then connected to form a three-phase transformer bank. Accounting for the effect of instrument transformers, the phase voltages and phase currents of the simulated three-phase transformer model were made available at the real-time simulator's output panel. A similar model was constructed and validated by [7] by comparing the models output during inrush, turn-to-turn faults, and overexcitation to expected values.

The analog-to-digital converter (ADC) circuitry, as described in Reference [8], was used to digitize the transformer's primary and secondary phase voltages and phase currents output by the real-time simulator at a rate of 1,920 Hz. The sampled voltage and current data were transfered to a PIC32MX360F512L micro-controller running at 80 Mhz. This micro-controller buffered the incoming data, digitally processed it and applied the relay algorithm. An algorithm for raw data collection was also written to allow for the verification of the transformer model's output.

In order to verify the model constructed, the expected value of inrush current was calculated using the iterative procedure given in [9] and according to the example given in [10]. This calculation provided the maximum inrush current envelope that can be developed by the transformer under study.

This paper discusses the development of a transformer protection algorithm which uses negative-sequence voltage to detect turn-to-turn faults during energization and negative-sequence current during normal transformer operation.

Section II discusses power transformer turn-to-turn faults and briefly discusses methods used to detect these types of faults. Section III describes the proposed negative-sequence-based scheme. Section IV describes the relay prototype and how it was tested. Section V provides the prototype test results.

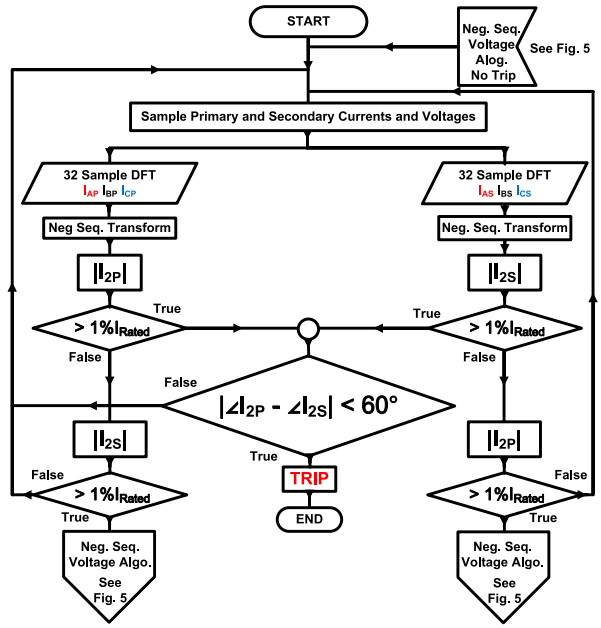

Fig. 3. Proposed Algorithm: Negative-Sequence Current.

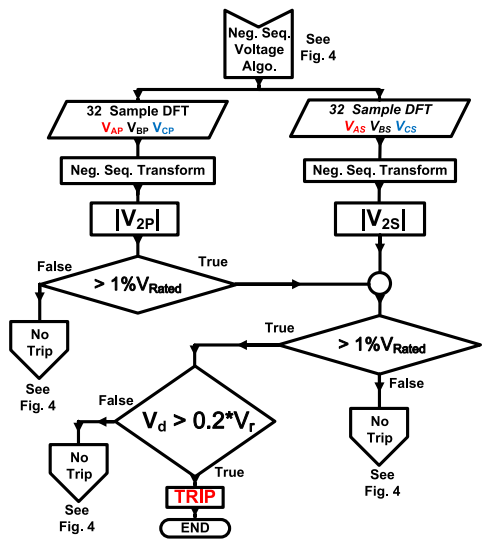

Fig. 4. Proposed Algorithm: Negative-Sequence Voltage Algorithm.

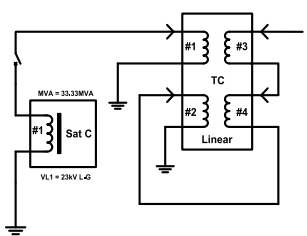

Fig. 5. RSCAD Model of a Nonlinear 4 Winding Transformer.

II. Detecting Turn-to-Turn Faults

A. Transformer Protection With Negative-Sequence Current

Negative-sequence current protection is in use in commercially available transformer protection relays such as described in Reference[11]. This relay makes use of a negative-sequence

percentage differential current element which is calculated by the vector addition of all currents entering the protection zone. The algorithm is sensitive enough to detect faults involving 2% of the transformer's windings. However, during inrush conditions, this relay blocks the negative-sequence current differential element.

The relay described in Reference[12] makes use of the primary and secondary negative-sequence currents along with their phase difference. Fig. 1 describes this algorithm visually. Both primary and secondary negative-sequence current magnitudes must be larger than $I_{\min}$ in order for a phase comparison to occur. If either or both negative-sequence currents is less than $I_{\min}$, the phase is set to 120°. This angle is outside the Relay Operating Angle (ROA) and ensures no trip signal is issued if the negative-sequence current is too small to obtain an accurate phase angle. If the negative-sequence currents magnitudes are larger than $I_{\min}$, the phase difference between the primary and secondary negative-sequence currents is examined. This phase difference must fall within the region described by the ROA.

III. Negative-Sequence-Based Scheme

A. Negative-Sequence Current Scheme

A negative-sequence current-based algorithm (NSCA) for sensing turn-to-turn faults is proposed in [3]. First, the negative-sequence current is calculated for both the primary side and secondary side of the transformer. Two negative-sequence current phasors are obtained from the above analysis. Let $\vec{I}_{2P}$ and $\vec{I}_{2S}$ denote the negative-sequence current phasors calculated for the primary and secondary side of the transformer. The next step of this algorithm is to check the magnitudes of $\vec{I}_{2P}$ and $\vec{I}_{2S}$ to ensure that they are both above a minimum threshold as shown in (1) and (2). This is important not only to prevent false tripping due to minor imbalances but also to ensure that the phase angle of the negative-sequence currents are reliable.

$$| \vec{I}_{2P} | > 1\% \text{ Primary Base Current} \tag{1}$$

$$| \vec{I}_{2S} | > 1\% \text{ Secondary Base Current.} \tag{2}$$

Phases of $\vec{I}_{2P}$ and $\vec{I}_{2S}$ are compared if the magnitudes satisfy the above equations. If (3) is also satisfied, a trip is warranted. The current transformers (CT) are arranged such that negative-sequence current caused by external faults result in phase differences of 180°. Ideally, an internal fault would result in a 0° phase difference. CT saturation is the main cause of excursions from the ideal phase difference [3], making it necessary to allow for a range of angles from 0° to 60°. This may be visualized by setting the relay operating angle (ROA) equal to 60° in Fig. 1

$$| \angle(\vec{I}_{2P}) - \angle(\vec{I}_{2S}) | < 60°. \tag{3}$$

B. Proposed Method

The requirement that both (1) and (2) be satisfied for a valid phase comparison is an inherent weakness of the algorithm proposed in [3]. Both primary and secondary negative-sequence current magnitudes must be greater than the threshold described in (1) and (2) in order for a reliable phase comparison between primary and secondary negative-sequence currents. Transformer inrush can occur in situations where current is flowing on the primary and secondary sides of the transformer such as during the removal of a fault or the energization of a parallel transformer [13]. During the switching-in of a transformer's primary, with its secondary switch open, no current flows in the transformer's secondary windings while an inrush current appears on the primary windings causing the negative-sequence current-based turn-to-turn fault detection method to block for any severity of fault. The stresses of energization make the transformer particularly vulnerable to turn-to-turn faults [2]. This deficiency of the negative-sequence current algorithm will be addressed in this section.

A turn-to-turn fault not only affects the currents seen at a transformer's terminals, but also the voltages. A turn-to-turn fault changes the transformer's turns ratio as turns are bypassed by the fault. This causes a voltage imbalance amongst the phases. A nonzero negative-sequence current or voltage appears should an imbalance appear in a three-phase system. The negative-sequence current method of turn-to-turn fault detection is excellent when the transformer is loaded. But as there is no load current flowing during energization, this method is blind to turn-to-turn faults.

Voltage exists on the load side of the transformer whether current is flowing or not. The terminal voltages, while affected by inrush current, are less distorted by second harmonic [14] allowing the negative-sequence voltage algorithm to react faster to turn-to-turn faults than the current differential algorithm. When the primary phase voltages and secondary phase voltages are available, the negative-sequence voltages for the primary and secondary side of the transformer can be calculated. The algorithm for comparing these two negative-sequence voltages is similar to the differential current algorithm. The pick-up negative-sequence voltage is set to 1% of the rated phase voltage.

In order to illustrate how a voltage imbalance is detected, a single phase transformer with a turn-to-turn fault will be discussed in detail. It represents one phase of a 3-phase transformer experiencing a turn-to-turn fault. Two scenarios will be discussed: a turn-to-turn fault on the primary side or a turn-to-turn fault on the secondary side. The primary side turn-to-turn fault is shown in Fig. 2. A small portion of the primary windings are shorted causing a small amount of additional current i_p to be drawn. For example, a 1% turn-to-turn fault caused a 5.8% increase in phase current draw.

This does not create a significant change in e_p since the source resistance is assumed to be low. Therefore the negative-sequence voltage contributed by the primary side, given by V_{2_P} in (4), will be negligible

$$\begin{bmatrix} \vec{V}_{0_P} \\ \vec{V}_{1_P} \\ \vec{V}_{2_P} \end{bmatrix} = \frac{1}{3} \begin{bmatrix} 1 & 1 & 1 \\ 1 & a & a^2 \\ 1 & a^2 & a \end{bmatrix} \begin{bmatrix} \vec{V}_{a_P} \\ \vec{V}_{b_P} \\ \vec{V}_{c_P} \end{bmatrix}. \tag{4}$$

The current travelling through the short circuit changes the mmf contribution of the faulted winding causing a change in the effective turns ratio from N_p to N_p'. Therefore the secondary side contributes a large amount of negative-sequence voltage, as

given by V_{2_S} in (6). The two negative-sequence voltage magnitudes V_{2_P} and V_{2_S} are compared in a manner similar to differential current protection. Equation (4), (5), (6), and (7) are valid for Y-Y connected transformers.

$$V_s' = \frac{N_p'}{N_s} V_p \tag{5}$$

$$\begin{bmatrix} \vec{V}_{0_S} \\ \vec{V}_{1_S} \\ \vec{V}_{2_S} \end{bmatrix} = \frac{1}{3} \begin{bmatrix} 1 & 1 & 1 \\ 1 & a & a^2 \\ 1 & a^2 & a \end{bmatrix} \begin{bmatrix} \vec{V}_{a_S} \\ \vec{V}_{b_S} \\ \vec{V}_{c_S} \end{bmatrix}. \tag{6}$$

Similarly the secondary side turn-to-turn fault will change the effective turns ratio, from N_s to N_s', on the secondary side causing a change in the secondary voltage of the faulted phase as shown in (7). Therefore (6) will yield a nonzero negative-sequence voltage as an imbalance in voltage amongst phases is present. A fault on the primary side causes a decrease in secondary phase voltage while a fault on the secondary side causes an increase in phase voltage. Both scenarios caused an imbalance with respect to other phase voltages, resulting in negative-sequence voltage.

$$V_s' = \frac{N_p}{N_s'} V_p. \tag{7}$$

C. Proposed Negative-Sequence Algorithm

Negative-sequence current, existing on the primary and secondary side of the transformer is considered first, as shown in Fig. 3. If the negative-sequence current magnitude, detected on both primary and secondary sides of the transformer, is above the prescribed threshold, a phase comparison is warranted. If negative-sequence current exists only on the primary side of the transformer but not on secondary side, the primary side of the transformer is being energized. In this case the algorithm proceeds to the negative-sequence voltage algorithm. An energization on the secondary side of the transformer also results in the selection of the negative-sequence voltage algorithm shown in Fig. 4.

The negative-sequence voltage algorithm takes as input the primary and secondary phase voltages. Only the magnitude of the primary and secondary negative-sequence voltage is of interest in this case. Notice that the secondary negative-sequence voltage is transformed to the primary side of the transformer. Both the primary negative-sequence voltage and the secondary negative-sequence voltage, transformed to the primary side of the transformer, must be larger than 1% of the rated primary voltage. This prevents erroneous tripping due to small imbalances found in an unfaulted transformer. The restraining and differential voltages are calculated using (8) & (9) respectively for a Y-Y connected transformer where "n" is the nominal turns ratio.

$$V_r = \frac{\mid V_{2_P} \mid + \mid V_{2_S} \mid \times n}{2} \tag{8}$$

$$V_d = \mid\mid V_{2_P} \mid - \mid V_{2_S} \mid \times n \mid. \tag{9}$$

If the differential voltage exceeds the restraining voltage equation, a trip is warranted. The algorithm shown in Fig. 4 is only executed under certain conditions outlined in Fig. 3. In other words, when the transformer's negative-sequence currents indicate that the transformer is being energized, negative-sequence voltages are used to determine if the transformer is experiencing a turn-to-turn fault.

Voltage changes due to on-load tap changer (OLTC) operations are not a concern as the negative-sequence voltage algorithm is only on-line during transformer energization.

IEEE standard [15] requires that the transformer winding voltages, at no load, be within 0.5% of the nameplate voltage. If a 0.5% imbalance is introduced to the otherwise healthy system, it produces a negative-sequence voltage well below the threshold.

IV. Verification of the Relay Prototype

A. Construction of a Relay Prototype

A prototype was constructed in order to test the novel method of turn-to-turn fault detection, valid during energization, proposed in Section III-B. In order to obtain current and voltage signals that can be processed by the prototype, a model of a three phase transformer was constructed using an RTDS™ Real Time Digital Simulator (RTDS) developed by RTDS Technologies [16]. These signals are then fed to the prototype which consists of an Analog to Digital Conversion (ADC) board and a Microchip micro-processor. The incoming signals were sampled at 1,920 Hz by the ADC and 10 consecutive samples of negative-sequence voltage/current terms were monitored in the PIC micro-controller for the trip criteria before generating a trip signal.

B. The RTDS Transformer Model

A transformer model with two major capabilities was required. First, a model capable of representing a transformer undergoing a turn-to-turn fault was required. Secondly, the nonlinear characteristics of the transformer's core had to be adequately represented during energization. A bank of three, magnetically independent single phase transformers was used for this purpose. As described by Yacamini *et al.* such a model is a good approximation to three-limb or five-limb transformer, whose phases are not magnetically independent, during inrush when the core is heavily saturated. During heavy saturation, the flux will flow in parallel air paths and will not be confined to the core [17]. This effectively isolates each phase magnetically.

C. Inclusion of Core Nonlinearity

Dommel reported the use of nonlinear inductances across the terminals of auto-transformers in order to simulate a nonlinear core [18]. Yacamini *et al.* describe the use of a nonlinear transformer bank in order to model a nonlinear three phase transformer [17]. Each phase is identical and consists of a nonlinear inductance in parallel with an ideal transformer as shown in Fig. 5.

The transformer core saturation curve can be approximated by two lines of different slopes [16], [18]. Two slopes allow for two states: saturated and unsaturated. Below the saturation curve's knee, the core is unsaturated and the magnetizing inductance is large. Above the knee, the core is saturated the magnetizing inductance is low.

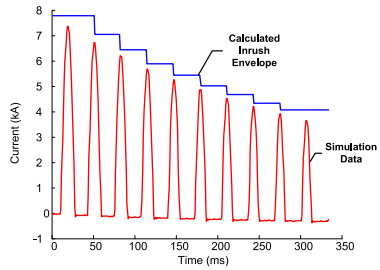

Fig. 6. Comparison of Calculated to Model Peak Inrush Current.

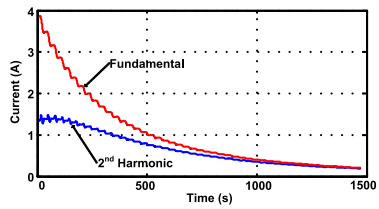

Fig. 7. Fundamental and Second Harmonic Current Data.

D. Verification of Inrush Current Model

To verify the model the expected value of inrush current was calculated using the iterative procedure given in [9] and according to the example given in [10]. This calculation provided the maximum inrush current envelope that can be developed by the transformer under study. These calculated peak values were compared to the values obtained from the RTDS model in Fig. 6. The iterative calculation, accurate for the first ten cycles [10], were used to find the inrush current envelope given below.

The fundamental and second harmonic current of inrush current data, collected from the unfaulted RTDS transformer model, is shown in Fig. 7. These waveshapes were compared to the fundamental and second harmonic current of inrush current data shown in [19].

V. Prototype Test Results

A. High Voltage Winding Fault During Steady-State

Turn-to-turn faults involving 1%, 3%, 5%, 10%, 15%, 25% of the high voltage winding were simulated consecutively. Given these conditions, the proposed method detected faults involving 3% of the high voltage windings or more. The primary and secondary negative-sequence current magnitudes are shown in Fig. 8, along with the phase difference between the two currents. The trip signal issued by the algorithm is shown in the lower frame of Fig. 8. The simulated fault occurred in phase C of the transformer. Line-to-ground and Line-to-Line faults, which are external sources of negative-sequence voltages, were used to test the proposed algorithm and resulted in no erroneous trips.

Negative-sequence phasor magnitudes were calculated using root mean square (RMS) line current. The trip delay times are summarized in the form of Table I for the proposed algorithm while the differential algorithm's trip delay time is given in Table II. For energization conditions, the trip delay times are summarized in the form of Tables III–IV.

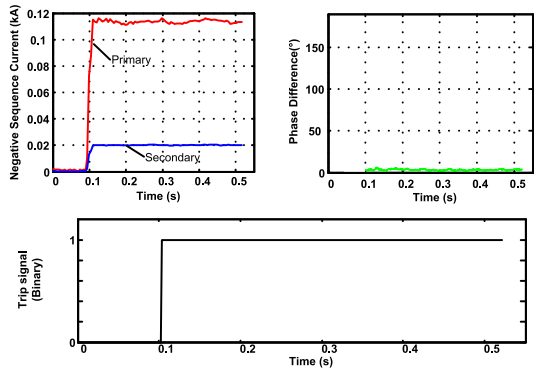

Fig. 8. Proposed Algo: 3% Turn-to-Turn Fault, Steady-State.

TABLE I
Neg. Seq. Algo: Steady-State, Fault on Phase C.

% Turns Faulted	Trip Time (ms)
1	No Trip
3	11.98
5	15.10
10	11.46
15	10.42
25	9.38

TABLE II
Diff. Algo: Steady-State, Fault Ph. C.

% Turns Faulted	Trip Time (ms)
1	No Trip
3	No Trip
5	No Trip
10	21.35
15	20.31
25	19.79

TABLE III
Neg. Seq. Algo: Inrush Ph. A, Fault on Ph. C.

% Turns Faulted	Trip Time (ms)
1	No Trip
3	102.08
5	35.42
10	21.35
15	21.35
25	19.27

TABLE IV
Diff. Algo: Inrush on Ph. A, Fault on Ph. C.

% Turns Faulted	Trip Time (ms)
1	No Trip
3	No Trip
5	No Trip
10	177.60
15	263.54
25	74.48

B. Current-Transformer Saturation

The negative-sequence-based relay performed well, detecting turn-to-turn faults occurring in phase C of the transformer, involving 1% to 25% of the windings. Trip delay times for the

TABLE V
NEG. SEQ. ALGO: 4.56 Ω CT BURDEN.

% Turns Faulted	Trip Time (ms)
1	15.63
3	11.46
5	12.50
10	10.94
15	11.98
25	9.90

TABLE VI
DIFF. ALGO: 4.56 Ω CT BURDEN.

% Turns Faulted	Trip Time (ms)
1	No Trip
3	No Trip
5	No Trip
10	21.35
15	20.31

TABLE VII
NEG. SEQ. ALGO: 1 Ω FAULT RESISTANCE.

% Turns Faulted	Trip Time (ms)
1	No Trip
3	22.40
5	16.15
10	15.10
15	11.46
25	9.90

TABLE VIII
DIFF. ALGO: 1 Ω FAULT RESISTANCE.

% Turns Faulted	Trip Time (ms)
1	No Trip
3	No Trip
5	No Trip
10	No Trip
15	20.83
25	20.31

proposed algorithm are tabulated in Table V. This is consistent with the findings in [3].

C. 1 Ω Turn-to-Turn Fault Resistance During Steady-State

For the following simulations, a fault having a resistance of 1 Ω was applied to the high voltage winding of the Phase C transformer. During steady-state, the negative-sequence-based algorithm detected faults involving 3% of the high-voltage windings or more. Trip times, tabulated in Table VII may be compared to Table I. Trip delay times observed for the differential relay, with a turn-to-turn fault resistance of 1 Ω, are given in Table VIII.

D. 1 Ω Turn-to-Turn Fault Resistance During Energization

Significant trip delays were introduced as a result of the 1 Ω fault resistance. But as can be seen in Table IX, the trip delay decreased remarkably with the 5% turn-to-turn fault and almost vanished for the 10% turn-to-turn fault.

E. 120% Overexcitation During Steady-State

Trip times collected at 120% overexcitation, as shown in Table XI, may be compared to trip times collected at rated voltage as given in Table I. The proposed algorithm was able to detect 1% turn-to-turn faults in the overexcited transformer since the negative-sequence currents on both the primary and

TABLE IX
NEG. SEQ. ALGO: 1 Ω FAULT RESISTANCE DURING ENERGIZATION.

% Turns Faulted	Trip Time (ms)
1	No Trip
3	233.85
5	78.13
10	21.35
15	15.63
25	19.27

TABLE X
DIFF. ALGO: 1 Ω FAULT RESISTANCE DURING ENERGIZATION.

% Turns Faulted	Trip Time (ms)
1	No Trip
3	No Trip
5	No Trip
10	328.13
15	244.27
25	20.31

TABLE XI
NEG. SEQ. ALGO: Y-Y: 120% OVEREXCITATION.

% Turns Faulted	Trip Time (ms)
1	13.02
3	11.46
5	11.46
10	15.10
15	9.90
25	9.38

TABLE XII
DIFF. ALGO: Y-Y: 120% OVEREXCITATION.

% Turns Faulted	Trip Time (ms)
1	No Trip
3	No Trip
5	100.52

TABLE XIII
NEG. SEQ. ALGO: Y-Y: 120% OVEREXCITED & INRUSH.

% Turns Faulted	Trip Time (ms)
1	No Trip
3	86.46
5	35.94
10	21.35
15	17.71
25	18.75

secondary sides of the transformer were above the minimum threshold. The negative-sequence phase difference showed a trip in both cases. The differential algorithm trip signal, given in Table XII, was delayed due to the overexcited state. The differential algorithm detected 5% and larger turn-to-turn faults.

F. 120% Overexcitation During Inrush

Energization occurred on the primary side in all cases described in this subsection with the most severe inrush occurring on phase A. In comparing trip times for energization at rated excitation voltage given in Table III with trip times of a 120% overexcited transformer given in Table XIII, there is little difference in trip times for most fault severities.

The differential algorithm appears sensitive to even 1% turn-to-turn fault, if overexcited by 120% of rated voltage, as shown in Table XIV. While this appears to be an improvement in sensitivity over the transformer operating at rated excitation,

TABLE XIV
DIFF. ALGO: Y-Y: 120% OVEREXCITED & INRUSH.

% Turns Faulted	Trip Time (ms)
1	302.60
3	428.13
5	377.60
10	294.79
15	228.13
25	20.83

TABLE XV
NEG. SEQ. ALGO: Δ-Y, ENERG. COMPARISON.

% Turns Faulted	No CCVT Trip Time (ms)	With CCVT Trip Time (ms)
1	276.04	No Trip
3	21.88	20.83
5	93.23	67.19
10	34.90	25.00
15	15.10	23.44
25	20.31	6.25

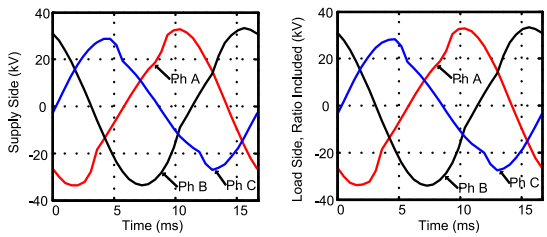

Fig. 9. CCVT Output Waveforms on Supply Side & Load Side of Transformer, 25% TT Fault.

given in Table IV, the differential relay was much slower in detecting turn-to-turn faults during energization when compared to the negative-sequence-based algorithm. In comparing Tables XIII and XIV, only a 25% turn-to-turn fault was detected with comparable speed using either the differential algorithm or the negative-sequence algorithm.

Overexcitation of a transformer, due to a sudden loss of load, would result in a significant amount of higher odd harmonics generated [20]. These harmonics may be used to restrain the proposed algorithm to prevent mal-operation given a transformer experiencing primary voltage imbalance and overexcitation simultaneously. The RTDS transformer model used to test the proposed algorithm was tested without residual flux present. The model can be extended to include residual flux as described in [21].

G. Effect of Coupling Capacitor Voltage Transformer (CCVT)

During energization the inrush current creates voltage harmonics due to the source's impedance. The inclusion of the CCVT causes the 1% turn-to-turn fault to go undetected while the trip times for other faults are lower as shown in Table XV.

Oscillations in the negative-sequence voltage signals, in Fig. 11, are the cause of this change in trip time. Fig. 9 shows the CCVT secondary voltages on the supply side of the transformer and the CCVT secondary voltages on the load side of the transformer (the waveforms shown are for a Y-Y configuration transformer without a 30° phase shift).

The most significant reduction in trip time occurs for a fault involving 25% of the turns on the high voltage side of the

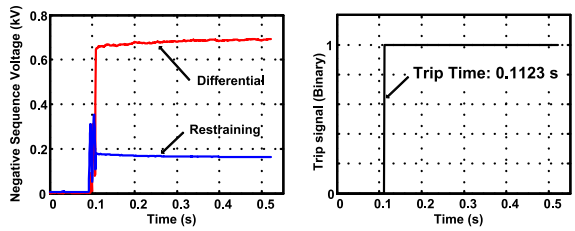

Fig. 10. Proposed Algo: 25% TT Fault during Energization without CCVT.

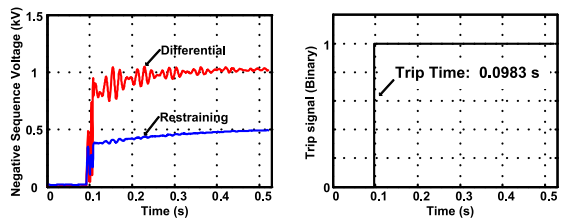

Fig. 11. Proposed Algo: 25% TT Fault during Energization with CCVT.

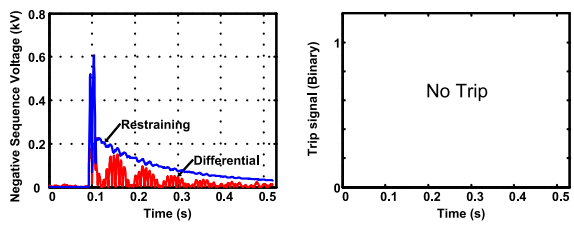

Fig. 12. Proposed Algo: Energization without Fault with CCVT.

TABLE XVI
LEAKAGE REACTANCES FOR HIGH-VOLTAGE SIDE FAULTS.

	25%	15%	10%	5%	3%	1%
X12	62.74	32.97	23.71	17.68	14.82	0.1196
X13	121.82	156.87	178.49	204.85	218.7	232.6
X14	66.40	109.88	141.92	184.82	207.73	230.64
X23	278.49	252.92	243.46	236.47	234.505	232.54
X24	162.34	181.61	194.02	210.83	221.195	231.56
X34	131.9	106.58	92.09	71.13	65.15	59.00

TABLE XVII
LEAKAGE REACTANCES FOR FAULTS ON LOW-VOLTAGE SIDE.

	25%	15%	10%	3%	1%
X12	71.38	36.97	25.6	16.87	7
X13	128.48	164.42	200.36	219.09	247.69
X14	69.55	113.14	156.73	204.4	234.097
X23	308.2	277.56	246.92	244.63	217.512
X24	178.16	196.4	214.64	222.14	237.056
X34	147.45	113.11	78.77	46.88	22.352

phase C transformer as shown in Fig. 11. This increased sensitivity comes at a price. The risk of false tripping is increased: Fig. 12 shows the negative-sequence voltage oscillations very close to the restraining voltage term during energization with the CCVT effect. The effect of these harmonics is shown in Table XV which compares trip times without a CCVT model and trip times with a CCVT model included. In both cases, the fault was initiated at 92 ms.

VI. CONCLUSION

The negative-sequence-based algorithm was consistently shown to be more sensitive and faster than the current dif-

ferential algorithm. This observation is supported by the experimental data. Turn-to-turn faults involving 3% of the transformer's windings were detected consistently by the proposed algorithm. The current differential algorithm with second harmonic restraint was able to detect turn-to-turn faults involving 10% of the transformer's windings under ideal conditions. The sensitivity of the differential current scheme was found to vary with CT saturation, fault resistance, and transformer overexcitation.

REFERENCES

[1] B. Kasztenny, E. Rosolowski, M. Saha, and B. Hillstrom, "A self-organizing fuzzy logic based protective relay-an application to power transformer protection," *IEEE Trans. Power Del.*, vol. 12, no. 3, pp. 1119–1127, Jul. 1997.

[2] A. Wiszniewski, W. Rebizant, and L. Schiel, "Sensitive protection of power transformers for internal inter-turn faults," in *Proc. IEEE PowerTech*, Bucharest, Romania, Jul. 28–2, 2009, pp. 1–6.

[3] Z. Gajic, I. Brncic, B. Hillstrom, and I. Ivankovic, "Sensitive turn-to-turn fault protection for power transformers," in *CIGRE, Study Committee B5 Colloq.*, Calgary, AB, Canada, 2005.

[4] M. Babiy, R. Gokaraju, and J. Garcia, "Turn-to-turn fault detection in transformers using negative sequence currents," in *Proc. IEEE Elect. Power Energy Conf.*, 2011, pp. 158–163.

[5] L. Underwood, *Setting 100% Stator Ground Fault Detection Elements in the SEL-300G Relay*. Pullman, WA, USA: Schweitzer Engineering Laboratories, 2005.

[6] Y. Kang, B. Lee, S. Kang, and P. Crossley, "Transformer protection based on the increment of flux linkages," *Proc. Inst. Elect. Eng., Gen., Transm. Distrib.*, vol. 151, no. 4, pp. 548–554, 2004.

[7] B. Kasztenny, E. Rosolowski, M. M. Saha, and B. Hillstrom, "A power transformer model for investigation of protection schemes," presented at the Int. Conf. Power Syst. Transients, Lisbon, Portugal, Sep. 1995.

[8] T. Sidhu, M. Sachdev, H. Wood, and M. Nagpal, "Design, implementation and testing of a microprocessor-based high-speed relay for detecting transformer winding faults," *IEEE Trans. Power Del.*, vol. 7, no. 1, pp. 108–117, Jan. 1992.

[9] T. R. Specht, "Transformer magnetizing inrush current," *Trans. Amer. Inst. Elect. Eng.*, vol. 70, no. 1, pp. 323–328, Jul. 1951.

[10] S. Kulkarni and S. Khaparde, *Transformer Engineering, Design and Practice*. New York, USA: Marcel Dekker, 2004.

[11] Schweitzer Engineering Laboratories, Pullman, WA, USA, SEL-487E transformer differential relay datasheet, Rep. no. PM487E-01, 2012.

[12] *"Transformer Protection RET650 Technical Manual,"* 1st ed. ABB, 2013.

[13] B. Kasztenny and A. Kulidjian, "An improved transformer inrush restraint algorithm increases security while maintaining fault response performance," presented at the 53rd Annu. Conf. Protect. Relay Eng., College Station, TX, USA, Apr. 2000.

[14] D. Povh and W. Schultz, "Analysis of overvoltages caused by transformer magnetizing inrush current," *IEEE Trans. Power App. Syst.*, vol. PAS-97, no. 4, pp. 1355–1365, Jul. 1978.

[15] *IEEE Standard General Requirements for Liquid-Immersed Distribution, Power, and Regulating Transformers, Std.*, Standard no. C57.12. 00-2000, 2000.

[16] *Real Time Digital Simulator Power System Users Manual*. Winnipeg, MB, Canada: RTDS Technologies, 2006, p. 398.

[17] R. Yacamini and A. Abu-Nasser, "The calculation of inrush current in three-phase transformers," *Proc. Inst. Elect. Eng., Elect. Power Appl.*, vol. 133, no. 1, pp. 31–40, Jan. 1986.

[18] , "Transformer models in the simulation of electromagnetic transients," presented at the 5th Power Syst. Comput. Conf., Cambridge, U.K., Sep. 1975.

[19] L. M. R. Oliveira and A. J. M. Cardoso, "Power transformers behavior under the occurrence of inrush currents and turn-to-turn winding insulation faults," in *Proc. XIX Int. Conf. Elect. Mach.*, 2010, pp. 1–7.

[20] G. W. Alexander, S. L. Corbin, and W. McNutt, "Influence of design and operating practices on excitation of generator step-up transformers," *IEEE Trans. Power App. Syst.*, vol. PAS-85, no. 8, pp. 901–909, Aug. 1966.

[21] A. Pors and N. Browne, "Modelling the energisation of a generator step-up transformer from the high voltage network," in *Proc. Austral. Univ. Power Eng. Conf*, Dec. 2008, pp. 1–5.

Daniel Zacharias received the B.Sc. degree in engineering physics and the M.Sc. degree in electrical engineering in from the University of Saskatchewan, Saskatoon, SK, Canada, in 2003 and 2014, respectively.

From 2003 to 2010, he was an Electronics Engineer in Saskatoon. Currently, he is an Electrical Engineer (P.Eng.) with Dynamo Electric. His areas of interest are power systems protection, relay testing, and maintenance.

Ramakrishna Gokaraju (S'88–M'00–SM'15) graduated in Electrical and Electronics Engineering from Regional Engineering College, Trichy, India, in 1992. He received the M.Sc. and Ph.D. degrees in electrical and computer engineering from the University of Calgary, Calgary, AB, Canada, in 1996 and 2000, respectively.

From 1999 to 2002, he was with the Alberta Research Council, Calgary, as a Research Scientist and the IBM Toronto Lab, Toronto, ON, as a Staff Software Engineer. He joined the University of Saskatchewan, Saskatoon, SK, Canada, in 2003 as an Assistant Professor and is currently a Professor at the university. His research is in power systems protection and control, and real-time simulations approaches.